

Document downloaded from:

<http://hdl.handle.net/10251/102622>

This paper must be cited as:

García-Ivars, J.; Martella, L.; Massella, M.; Carbonell Alcaina, C.; Alcaina-Miranda, Ml.; Iborra Clar, Ml. (2017). Nanofiltration as tertiary treatment method for removing trace pharmaceutically active compounds in wastewater from wastewater treatment plants. *Water Research*. 125:360-373. doi:10.1016/j.watres.2017.08.070



The final publication is available at

<http://dx.doi.org/10.1016/j.watres.2017.08.070>

Copyright Elsevier

Additional Information

1 **Nanofiltration as tertiary treatment method for removing**
2 **trace pharmaceutically active compounds in wastewater from**
3 **wastewater treatment plants**

4
5 Jorge Garcia-Ivars ^{a, *}, Lucia Martella ^b, Manuele Massella ^c, Carlos Carbonell-Alcaina ^a,
6 Maria-Isabel Alcaina-Miranda ^{a, d}, Maria-Isabel Iborra-Clar ^{a, d}

7
8 ^a Research Institute for Industrial, Radiophysical and Environmental Safety (ISIRYM), Universitat
9 Politècnica de València, C/Camino de Vera s/n, 46022 Valencia, Spain

10 ^b Dipartimento di Ingegneria Civile, Chimica, Ambientale e dei Materiali (DICAM), Università di
11 Bologna, Via Terracini, 28, 40131 Bologna, Italy

12 ^c Dipartimento di Ingegneria Civile, Edile e Ambientale, Università Sapienza di Roma, Via Eudossiana
13 18, 00184 Rome, Italy

14 ^d Department of Chemical and Nuclear Engineering, Universitat Politècnica de València, C/Camino de
15 Vera s/n, 46022 Valencia, Spain

16
17 **Keywords:**

18 Pharmaceutically active compounds; Nanofiltration; Rejection efficiency; Fouling
19 mechanisms; Phenomenological model.

20
21 **Abstract**

22
23 The ever-increasing occurrence and persistence of pharmaceutically active compounds
24 (PhACs) in soils, sediments, drinking water supplies and wastewater effluents are a
25 matter of serious environmental concern for governments and researchers worldwide.
26 Nanofiltration as tertiary treatment method can be a viable and practical tool to remove
27 these pollutants from aquatic environments. However, organic matter present in water
28 sources can foul the membrane surface during operation, thus being potentially able to
29 affect the membrane performance. Therefore, fouling mechanisms could heavily
30 influence on the removal efficiencies. The purpose of this study was to investigate the
31 implementation of three nanofiltration membranes (TFC-SR2, NF-270 and MPS-34)
32 and to study both the rejection of trace PhACs and the fouling mechanisms for each
33 membrane as a function of feed solution pH. Fouling mechanisms were predicted by
34 Hermia's model adapted to cross-flow configurations. Results demonstrated that higher

35 removals were obtained at slightly alkaline pH, especially for anionic trace PhACs. At
36 the same conditions, more severe fouling was observed, which resulted in strong flux
37 declines and an increase in hydrophobicity. This indicates that the attached organic
38 matter on the membrane surface acts as a secondary selective barrier for separation.

39

40 **1. Introduction**

41

42 An extremely increasing presence of emerging contaminants and in particular
43 pharmaceutically active compounds (PhACs) has been detected at trace concentration
44 (ranging from ng/L up to several mg/L) as free compounds and/or as metabolites in
45 many environmental matrices worldwide, including drinking water supplies, wastewater
46 effluents and soils and sediments (Heberer, 2002; Verlicchi et al., 2012; Wang and
47 Wang, 2016; Smith Jr., 2014). This growing occurrence and persistence in soils and
48 aquatic environments, together with their diversity, make them some of the most
49 targeted compounds to be removed. In the last decades, pharmaceuticals have been
50 extensively used in large quantities but they are incompletely absorbed and metabolised
51 by human and animal organism, thus resulting in non-absorbed and non-metabolised
52 portions which are disposed of in the environment through their excretions (urine and
53 faeces) (Picó and Barceló, 2015; Archer et al., 2017). The potential health risks
54 associated with the release of these pollutants into the environment and their completely
55 possible interactions with living organisms are a matter of serious environmental
56 concern for national/international scientific communities, governments and regulatory
57 agencies (Verlicchi and Zambello, 2015; Jung et al., 2015; Grandclément et al., 2017).

58

59 PhACs are synthetic organics designed with the objective of enhancing human
60 health standards. However, their continuous discharge to aquatic environment may
61 cause unwanted side effects on non-target living organisms. Some examples of such
62 side effects would be human and wildlife reproduction disorders and the development
63 and proliferation of antibiotic-resistant bacteria, mainly due to many of them are
64 recalcitrant to biodegradation and prone to bioaccumulation (Halling-Sorensen et al.,
65 1998; Schmidt et al., 2012; Petrie et al., 2015). Due to their ubiquitous and
66 nonbiodegradable character, pharmaceutical residues cannot be completely removed or
67 degraded in conventional wastewater treatment plants (WWTPs) and PhACs are
68 released into the environment, thus making the secondary effluents discharged from

69 WWTPs into a major source of pharmaceutical micropollutants (Chon et al., 2013;
70 Grandclément et al., 2017). In some cases, their concentration has increased after
71 passing through conventional wastewater treatment due to their transformation into
72 conjugates (Vergili, 2013). This situation has led researchers to explore new treatment
73 strategies as tertiary processes to efficiently remove PhACs from secondary effluents
74 from WWTPs, such as activated carbon adsorption, advanced oxidation processes using
75 ozone and hydroxyl radicals or membrane technology.

76

77 As a well-established sustainable technology for removing natural organic
78 matter, macromolecules, colloids, pathogens and turbidity, membrane technology is
79 increasingly applied in municipal and industrial wastewater treatment as an affordable
80 alternative for sustainable water reclamation/reuse. Several studies employing
81 ultrafiltration (UF), nanofiltration (NF) and reverse osmosis (RO) have been carried out
82 to investigate the removal mechanisms and efficiencies of PhACs using membrane
83 separation processes. In addition to the fouling phenomena and their detrimental effect
84 on the lifespan and performance of membranes, which has been extensively reported by
85 different researchers (Li and Elimelech, 2004; Van der Bruggen et al., 2008; Kochkodan
86 and Hilal, 2015), the presence of natural organic matter (NOM) during membrane
87 filtration can lead to a competition with PhACs and other micropollutants in the aquatic
88 environment for the adsorption sites on the membrane surface, thus causing lowered
89 adsorption rates of these low-molecular weight compounds (Jermann et al., 2009). This
90 situation can also occur when activated carbon adsorption is used as alternative removal
91 technique (Altmann et al., 2014). Previous studies demonstrated that the existing
92 interactions between organic matter and PhACs can help remove them from aquatic
93 environments, either as a part of the retentate stream or as a solute adsorbed on the
94 membrane, especially due to the hydrophobic interactions between organic matter and
95 PhACs and the adsorptive mechanism (Khansary et al., 2017; García-Ivars et al., 2017).
96 Extensive studies demonstrated that nanofiltration have been efficiently implemented to
97 remove PhACs and other micropollutants, but many of them were focused on its
98 application in synthetic model waters where the target compounds were spiked (Nghiem
99 and Hawkes, 2007; Comerton et al., 2009; Dolar et al., 2013; Lin et al., 2014) and very
100 few of them were concentrated on its implementation in real wastewaters, rivers or
101 drinking water production (Snyder et al., 2007; Bellona et al., 2010; Azaïs et al., 2016).

102

103 In this work, the role of feed solution and its constituents in the removal of
104 PhACs with different physicochemical properties and the personal care product
105 triclosan from real wastewater by using NF cross-flow membranes was studied. The
106 performance of three different membranes from very loose to tight NF within the pH
107 range from 6 to 8 was evaluated in terms of permeate flux and rejection indexes of each
108 target compound. The present work include the personal care product triclosan and eight
109 selected PhACs which represented the most common PhACs found in WWTP
110 secondary effluents at the Spanish Mediterranean area of Valencia, being found
111 acetaminophen, ibuprofen and sulfamethoxazole in concentrations ranging from 20 ng/L
112 to several mg/L (in the worst case scenario, up to 20-100 mg/L) and the rest of target
113 compounds in lower concentration ranges from 1 to 2-4000 ng/L ([Gracia-Lor et al.,](#)
114 [2012](#); [Pascual-Aguilar et al., 2015](#), [Picó and Barceló, 2015](#)). As a novelty, fouling
115 mechanisms at each pH condition for each NF membrane were predicted by Hermia's
116 model adapted to cross-flow configurations. The predominant fouling mechanisms at
117 the studied conditions were related to the mechanism for which each target compound
118 was rejected. The rejection indexes of the selected emerging contaminants were
119 determined by the composition of both feed and permeate streams of the process via
120 High-Performance Liquid Chromatography (HPLC).

122 **2. Materials and methods**

124 **2.1. WWTP secondary effluent samples**

126 Secondary effluent samples were obtained from a municipal WWTP located in
127 the region of Valencia (Carraixet WWTP, Spain). Their characterisation was carried out
128 according to the standard methods defined by the American Public Health Association
129 to examine the characteristics of water and wastewater ([APHA, 2012](#)) and the results
130 are summarised in [Table 1](#). The samples of this secondary effluent have an alkaline pH
131 with a high electrical conductivity, turbidity and moderate COD and BOD parameters in
132 comparison with researchers who used secondary effluents ([Katsoyiannis et al., 2017](#);
133 [Chon et al., 2017](#)).

135
136

Table 1. Water quality parameters of the selected secondary effluents from a local waste-water treatment plant at 25°C.

Parameter	Average result \pm standard deviation
pH	8.41 \pm 0.10
m-Alkalinity (mg CaCO ₃ /L)	415.52 \pm 19.34
Electrical conductivity (μ S/cm)	1406.00 \pm 71.06
TSS (mg/L)	363.73 \pm 69.79
Turbidity (NTU)	35.46 \pm 3.41
COD (mg O ₂ /L)	94.77 \pm 5.37
BOD (mg O ₂ /L)	11.71 \pm 1.87
UV ₂₅₄	0.283 \pm 0.003
Ca ²⁺ (mg/L)	76.61 \pm 3.84
Mg ²⁺ (mg/L)	25.17 \pm 1.04
Cl ⁻ (mg/L)	185.89 \pm 0.64
Total Nitrogen (mg N/L)	73.30 \pm 16.10
Proteins (mg/L)	65.25 \pm 10.03

137
138

139 2.2. Chemicals

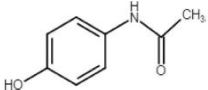
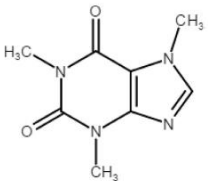
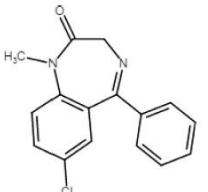
140

141 High purity standards (>99%) of acetaminophen, caffeine, diazepam, diclofenac,
142 ibuprofen, naproxen, sulfamethoxazole, triclosan and trimethoprim were purchased
143 from Sigma-Aldrich (Germany) and were used without further purification. The
144 physicochemical properties of the selected PhACs are summarised in [Table 2](#).

145

146

Table 2. Physicochemical properties of the nine PhACs employed in this study.

Pharmaceutical active compound	CAS no.	Molecular structure	Molecular weight (g/mol)	pK _a ^a	Log K _{ow} ^{ab}	Dipole moment (D) ^c	Molar volume (cm ³ /mol) ^c	Molecular radius (nm)	Diffusion coefficient (cm ² /s)
Acetaminophen	103-90-2		151.17	9.86	0.49 (Hydrophilic)	3.85	121.0	0.32	7.63 · 10 ⁻⁶
Caffeine	58-08-2		194.19	10.40	-0.04 (Hydrophilic)	3.40	133.9	0.36	6.80 · 10 ⁻⁶
Diazepam	439-14-5		284.75	3.40	2.82 (Hydrophobic)	2.17	226.0	0.43	5.70 · 10 ⁻⁶

147

Diclofenac	15307-79-6		318.14	4.08	4.64 (Hydrophobic)	2.51	207.0	0.45	$5.41 \cdot 10^{-6}$
Ibuprofen	15687-27-1		206.29	4.40	3.68 (Hydrophobic)	1.22	200.5	0.37	$6.61 \cdot 10^{-6}$
Naproxen	22204-53-1		230.27	4.15	2.82 (Hydrophobic)	2.84	192.4	0.39	$6.28 \cdot 10^{-6}$
Sulfamethoxazole	723-46-6		253.28	5.7	0.56 (Hydrophilic)	7.37	173.2	0.41	$6.01 \cdot 10^{-6}$
Triclosan	3380-34-5		289.55	7.8	5.53 (Hydrophobic)	2.45	194.3	0.43	$5.66 \cdot 10^{-6}$
Trimethoprim	738-70-5		290.32	6.6–7.1	0.98 (Hydrophilic)	2.54	231.9	0.43	$5.65 \cdot 10^{-6}$

148

149

150

151

152

153

154

155

156

157

158

159

160

161

162

^a SciFinder Scholar, data calculated at 20 °C and 760 torr using Advanced Chemistry Development (ACD/Labs) Software V11.02 (©1994e2016 ACD/Labs).

^b Hydrophobic when log K_{ow} >2.

^c Chem3D Ultra 8.0.

The logarithm of the octanol-water distribution coefficient (log K_{ow}) and acid dissociation constant (pKa) of each target compound were obtained from SciFinder Scholar database, whereas their volume of the solute (V_S , cm³ /mol) and dipole moment (M_{DIP} , Debyes) were determined using Chem3D Ultra 8.0 software. Additionally to these parameters, the hydrodynamic molecular radius or Stokes radius (r_s , m) of each compound was calculated using the Stokes-Einstein equation:

$$r_s = \frac{T \cdot k_B}{6 \cdot \pi \cdot \eta \cdot D_s} \quad (1)$$

163

164 where T is the absolute temperature (K), k_B is the Boltzmann constant ($\text{kg}\cdot\text{m}^2/(\text{K}\cdot\text{s}^2)$), h
165 is the viscosity of solvent ($\text{kg}/(\text{m}\cdot\text{s})$), and D_s is the diffusion coefficient of the organic
166 compound in water (m^2/s). The diffusion coefficient of the target emerging
167 contaminants (D_s) on aqueous solution can be approximated by the molecular weight
168 (M_W , g/mol) of the solute in accordance with the empirical equation
169 described by (Avdeef et al., 2004):

170

$$\log(D_s) = -4.113 - 0.4609 \log(M_W) \quad (2)$$

171

172

173 Solutions of 0.1 M HCl and 0.1 M NaOH were used to adjust the pH of feed
174 solutions. Both chemicals were obtained of reagent grade from Panreac (Spain).
175 Deionised water was used throughout the study.

176

177 **2.3. Membranes**

178

179 Three commercial spiral wound NF membranes were used in this investigation,
180 namely TFC-SR2, NF270, and SelRO MPS-34 A2X (henceforth MPS-34). The TFC-
181 SR2 and MPS-34 membranes with effective areas of 2.5 and 1.6 m^2 respectively were
182 supplied by Koch Membrane Systems (USA), whereas NF270 membrane with an
183 effective area of 2.6 m^2 was supplied by Dow FilmTec (USA). The selected membranes
184 span a wide range of molecular weight cut-off (MWCO), from loose to tight NF
185 membranes as follows: TFC-SR2 > NF-270 > MPS-34. Both NF-270 and TFC-SR2 are
186 considered as loose NF membranes with an estimated MWCO around 230-300 and 400
187 Da, respectively. Conversely, MPS-34 membrane can be defined as tight NF membrane
188 with a MWCO of 200 Da. Their main characteristics are given in Table 3. As it can be
189 observed, before the filtration experiments began, water permeability for each
190 membrane was calculated at different transmembrane pressure (ΔP , ranging from 2 to
191 10 bar), constant flow rate and operating temperature (500 L/h and 25 °C, respectively).

192

Table 3. Properties of the selected NF membranes.

Properties/Membrane	TFC-SR2	NF270	SelRO MPS 34 A2X
Manufacturer	Koch Membrane Systems	Dow FILMTEC™ Membranes	Koch Membrane Systems
Material chemistry	Proprietary Polyamide TFC® membrane	Polyamide Thin-Film Composite	Proprietary polysulfone composite membrane
Geometry	Spiral wound	Spiral wound	Spiral wound
MWCO (Da)	>300–400 350–460 ^{a,b}	230–300 ^{c,d,e}	200
Average pore radius (nm)	0.52–0.64 ^{a,b,f}	0.26–0.43 ^{c,g,h}	–
Water contact angle (°)	20–40 ^{i,j}	32–45 ^{g,h,k,l}	–75–80 ^m
Active surface (m ²)	2.5	2.6	1.6
Water permeability (L/m ² ·h·bar) ⁿ	17.7 ± 0.6	13.4 ± 0.2	1.1 ± 0.2
Maximum operating temperature (°C)	45	45	50
Maximum operating pressure (bar)	34.47	41	35
Allowable pH - continuous operation	4–9	2–11	0–14
Allowable pH - cleaning	2–11	1–12	0–14

^a Reported in (Nghiem and Hawkes, 2007); ^b Reported in (De Munari et al., 2013); ^c Reported in (Azais et al., 2014); ^d Reported in (Lopez-Muñoz et al., 2009); ^e Reported in (Lin et al., 2016); ^f Reported in (Nghiem et al., 2006); ^g Reported in (Nghiem and Coleman, 2008); ^h Reported in (Chang et al., 2011); ⁱ Reported in (Ali Zazouli et al., 2009); ^j Reported in (Bellona et al., 2010); ^k Reported in (Dražević et al., 2013); ^l Reported in (Owusu-Agyeman et al., 2017); ^m Reported in (Fernandez et al., 2010); ⁿ Deionised water flux was experimentally determined in this work at the following conditions: 2e10 bar, 25 °C, 500 L/h.

2.4. Experimental procedure

The filtration experiments were carried out in a laboratory scale cross-flow membrane filtration pilot plant equipped with a 2.5 inch AG 2540 spiral wound module. The feed solution was fed to the cross-flow system with a variable speed volumetric pump from a temperature-controlled feed tank with a capacity of 30 L. A pH meter was incorporated to the pump as well as two thermo immersion coolers (Haake® EK20, Thermo Electron Corporation, USA), which were used to control the operating temperature (25 ± 2 °C) and prevent an increase in water temperature resulting from using the pump. The transmembrane pressure was fixed at 5 bar using a stainless steel throttle valve on the retentate outlet and was monitored through two manometers located on the inlet and outlet of the membrane module. This low transmembrane pressure was selected mainly due to economic, energy and pressure vessel material savings. The use of such a transmembrane pressure (5 bar) to remove emerging contaminants (especially PhACs) from aquatic environments has been previously reported by other researchers (Yangali-Quintanilla et al., 2009; Yangali-Quintanilla et al., 2010; Miralles-Cuevas et al., 2017). Filtration experiments were performed at a constant flow of 500 ± 20 L/h, which was measured by a flow meter placed at the retentate outlet. The NF experiments operated in a total recirculation mode in which both concentrate and permeate streams were returned back to the feed tank to keep the feed concentration constant. Finally, a scale with an accuracy of ± 0.01 g was employed to gravimetrically measure the permeate flux.

224

225 Prior to each experiment, membranes were first stabilised by filtering deionised
226 water at 10 bar for at least 2 h until a stable water flux was reached. After that, filtration
227 experiments consisted in filtration runs of 4 h with WWTP secondary effluents where
228 target compounds were spiked (if necessary) to achieve the following initial
229 concentrations: 1000 ng/L of acetaminophen, ibuprofen and sulfamethoxazole and 300
230 ng/L of caffeine, diazepam, diclofenac, naproxen, triclosan and trimethoprim. The
231 experimental conditions were 500 ± 10 L/h, 5 bar and 25 ± 2 °C. The influence of pH
232 was tested at three pH levels from 6 to 8. The permeate flux (J_p , L/m²·h) was
233 determined by measuring the volume of permeate (V , L) collected at regular time
234 intervals (t , h) as follows:

235

$$J_p = \frac{V}{A_m \cdot t} \quad (3)$$

236

237

238 where A_m (m²) is the effective area of the membrane.

239

240 The rejection index (R , %) was calculated based on the concentration of each
241 PhAC in permeate (C_p , ng/L) and feed (C_f , ng/L) streams:

242

$$R(\%) = \frac{C_f - C_p}{C_f} \times 100 \quad (4)$$

243

244

245 In order to assess the fouling mechanism during the filtration of the WWTP
246 secondary effluent samples, the Hermia's model for constant pressure was selected. In
247 this model, Hermia distinguished four models for each predominant fouling mechanism:
248 gel layer formation, incomplete or intermediate blocking, standard blocking and
249 complete blocking (Hermia, 1982). The adaptation of such a model to cross-flow
250 configurations by incorporating the flux associated with the back transport mass transfer
251 (evaluated at the steady state) was developed by several authors (Field et al., 1995;
252 Vincent-Vela et al., 2009) and its general differential equation is the following
253 expression:

254

$$-\frac{dJ_p}{dt} = K \cdot (J_p - J_{pss}) \cdot J_p^{2-n} \quad (5)$$

255

256

257 where J_{pss} is steady-state permeate flux (same units as J_p), K is a phenomenological
 258 model constant with physical meaning and n is the model parameter, which depends on
 259 the fouling mechanism. Thus, when the value of n is 0 represents the formation of a gel
 260 layer by the accumulation of solute particles onto the membrane surface with a
 261 thickness proportional to the permeated volume. In this case, the pore blocking is
 262 neglected (Vincent-Vela et al., 2009). However, when n is 1, the fouling mechanism
 263 corresponds to the incomplete or intermediate blocking model in which the solute
 264 particles cannot penetrate completely inside the porous structure and then can settle on
 265 other particles deposited before, forming multilayers. The standard blocking model
 266 (with a value of n of 1.5) assumed that solute particles with a smaller size than the pores
 267 of the membranes can pass through the membrane pores and precipitate on inner pore
 268 walls, thus reducing the effective pore size. Finally, if n corresponds to 2, the complete
 269 blocking model is assumed. In this case, the size of the solute particles is similar to the
 270 pore size of the membrane, which results in that each solute particle participates in
 271 sealing the pore entrance without passing through the porous structure, thus forming a
 272 monomolecular layer on membrane surface (Corbatón-Báguena et al., 2016; Carbonell-
 273 Alcaina et al., 2016). The general representing equations for each fouling mechanism
 274 are the following expressions:

275

- Gel layer formation ($n = 0$):

277

$$t = \frac{1}{K_{GL} \cdot J_{pss}^2} \cdot \left[\ln \left(\frac{J_p \cdot J_0 - J_{pss}}{J_0 \cdot J_p - J_{pss}} \right) - J \cdot \left(\frac{1}{J_p} - \frac{1}{J_0} \right) \right] \quad (6)$$

278

279

- Incomplete or intermediate blocking ($n = 1$):

281

$$J_p = \frac{J_0 \cdot J_{pss} \cdot e^{K_{IB} \cdot J_{pss} \cdot t}}{J_{pss} + J_0 \cdot (e^{K_{IB} \cdot J_{pss} \cdot t} - 1)} \quad (7)$$

282

283

284 • Standard blocking (n = 1.5):

285

$$J_p = \frac{J_0}{\left(1 + J_0^{1/2} \cdot K_{SB} \cdot t\right)^2} \quad (8)$$

286

287

288 • Complete blocking (n = 2):

289

$$J_p = J_{pss} + \left(J_0 - J_{pss}\right) \cdot e^{-K_{CB} \cdot J_0 \cdot t} \quad (9)$$

290

291

292 2.5. Analytical methods

293

294 The extraction of the target compounds was based on solid-phase extraction
295 (SPE) in accordance with (Vazquez-Roig et al., 2011). Analytes were isolated from
296 water samples (250 mL, pH 7) using a polymeric Strata-X 33 mm Polymeric Reversed
297 Phase cartridge (200 mg/6 mL, Phenomenex, France) preconditioned with 5 mL of
298 methanol and 5 mL of Milli-Q water, and then eluted with methanol. The determination
299 of the different concentrations was performed by a HPLC-MS/MS system, where the
300 HPLC system (1260 Infinity Ultra, Agilent Technologies, USA) was coupled to an
301 LC/MS spectrometer (6410 Triple Quadruple Mass Spectrometer, Agilent
302 Technologies, USA) with an electrospray Turbo V ionisation source. Separation was
303 achieved on a Kinetex C18 column (1,7 mm; 50 mm × 2.1 mm; Phenomenex, France)
304 with the mixture of water/ methanol 70:30 (v/v) as the mobile phase. The flow rate and
305 injection volume were 0.2 mL/min and 20 mL, respectively. The mobile phase gradient
306 started from a 30-95% of methanol in 12 min, which maintaining for 8 min. After that,
307 the mobile phase returned to the initial conditions with an equilibrium time of 12 min
308 (Carmona et al., 2014).

309

310 2.6. Method validation

311

312 Seven-point calibration curves using standard and matrix-matched solutions
 313 (from the limit of quantification, LOQ, to 3 mg/ L) were obtained with a linear
 314 correlation coefficient $R^2 > 0.95$. These calibration standards were injected in triplicate.
 315 After the SPE method on water samples, the limits of detection (LODs) and LOQs were
 316 determined as the analyte concentration added to the water sample that produced in the
 317 extracted chromatogram of the transition used for quantification a peak signal of 3 and
 318 10 times in the background noise, respectively. The results were displayed in a previous
 319 work (García-Ivars et al., 2017). The method LODs were between 0.3 and 5 ng/L,
 320 whereas LOQs were from 1.0 to 15 ng/L.

321

322 3. Results and discussion

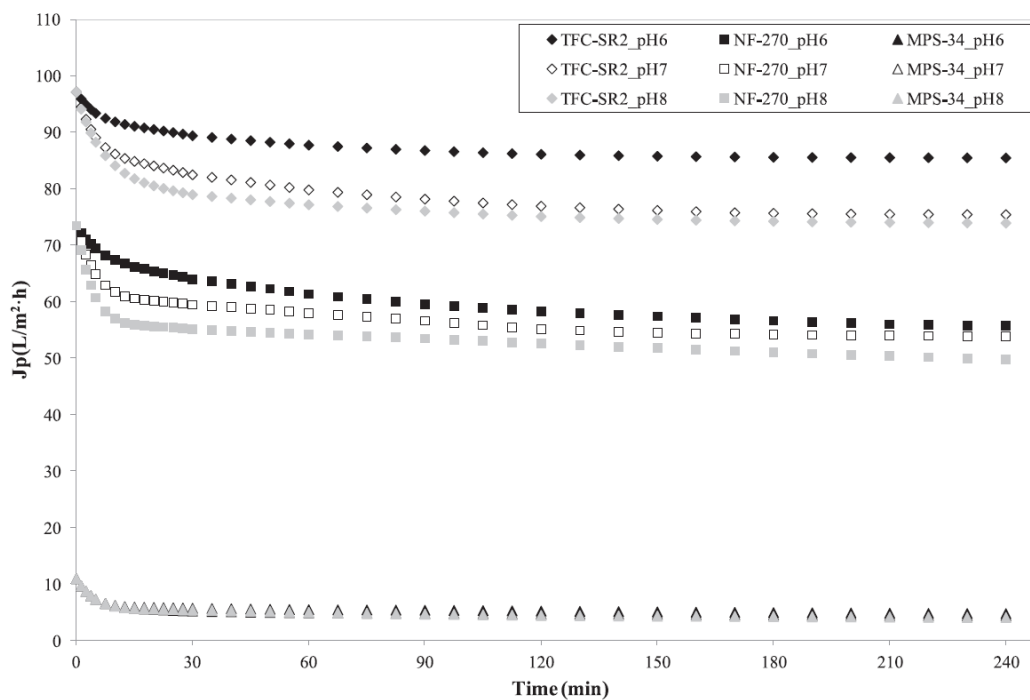
323

324 3.1. Fouling mechanisms

325

326 Fig. 1 shows the decline of the permeate flux (J_p) for each nanofiltration
 327 membrane during the filtration of the WWTP secondary effluent at the studied pH range
 328 (from 6 to 8).

329



330

331

332

333

Figure 1. Evolution of the permeate flux J_p over filtration time for each NF membrane at different pHs. Experimental conditions: 5 bar, 500 ± 20 L/h, and 25 ± 2 °C.

334 As expected, NF membranes with larger MWCO (loose NF membranes) showed
335 higher permeate flux in the whole pH range than tighter membranes, thus indicating that
336 the differences amongst NF membranes in terms of pore size and materials have a
337 remarkable influence in the permeate flux. The TFC-SR2 membranes presented a more
338 open porous structure (the highest MWCO of the selected membranes) and hence,
339 showed the highest permeate flux (84.54, 75.49 and 74.00 L/m²·h for pH 6, 7 and 8
340 respectively) whereas MPS-34 membranes (a tight NF membrane) showed the lowest J_p
341 value (4.78, 4.39 and 4.07 L/m²·h for the same pH values).

342

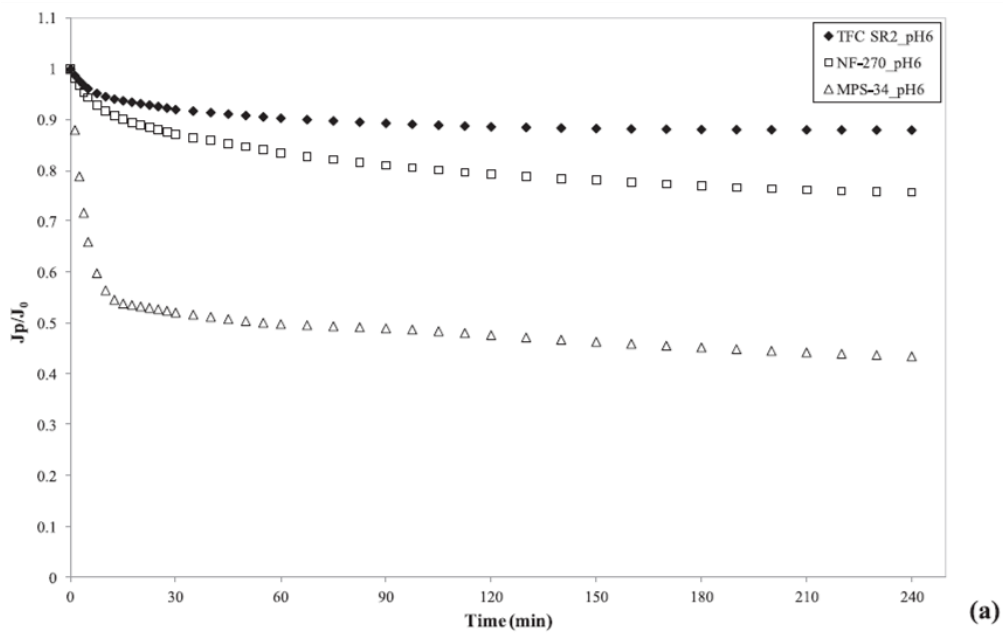
343 Two distinct stages can be distinguished in [Fig. 1](#) and evidenced the membrane
344 fouling: firstly, a rapid decrease of the permeate flux at low time scales in which the
345 retained solute particles were accumulated and adsorbed onto the surface and inside the
346 pore walls; and a subsequent and gradual flux decline at longer time periods, where the
347 equilibrium between the attachment and detachment of solute particles on the
348 membrane was reached, achieving an almost constant value of J_p (which will be
349 considered as steady-state flux or J_{pss}). Based on the quality of the secondary effluent
350 (see [Table 1](#)), the main cause of the observed flux decline is the adsorption and
351 deposition of effluent organic matter (EfOM) onto the membrane surface, which is
352 mainly evidenced by the values of COD, BOD, total nitrogen and proteins.

353

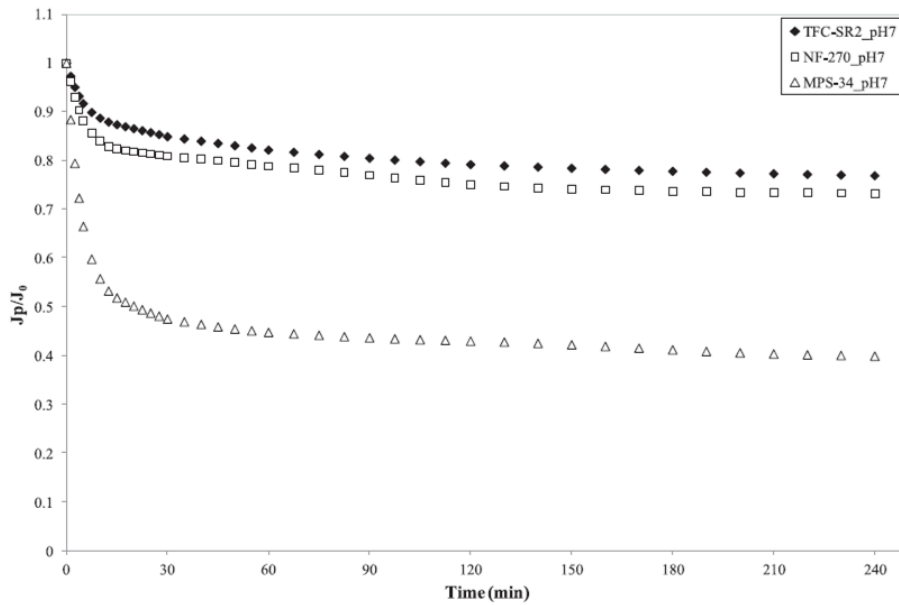
354 The effect of pH on fouling propensity can be clearly seen in [Fig. 2](#), where the
355 flux declines of each NF membrane at each pH condition (represented as normalised
356 flux J_p/J_0) as a function of time is displayed. All NF membranes were negatively
357 charged at the investigated pH range due to the fact that their isoelectric point or zero-
358 point of charge was 4 or lower, as was reported by several authors who characterised the
359 selected membranes ([Nghiem et al., 2006](#); [Nghiem and Hawkes, 2007](#); [López-Muñoz et al., 2009](#);
360 [Fernández et al., 2010](#); [De Munari et al., 2013](#); [Azaïs et al., 2014](#); [Owusu-
361 Agyeman et al., 2017](#)). The pH had a significant influence on the permeate flux which
362 decreased with increasing pH for each membrane. The charge variation of the
363 membrane surface is a key factor to predict its behaviour and it strongly depends on the
364 pH of the feed solution because the functional groups on the polymeric surface structure
365 are pH dependent. In the case of polyamide NF membranes, the presence of carboxylic
366 and amine functional groups on their active layer makes NF membranes susceptible to
367 be ionised when pH changes. The ionisation of such groups is reflected in the variation

368 of the zeta potential of the membrane surface with increasing and decreasing pH
369 conditions (Nghiem and Hawkes, 2007; Chang et al., 2011; Al-Rashdi et al., 2013). The
370 negative zeta potential of the polymeric NF membranes was higher with increasing pH
371 (from 6 to 8), which resulted in more negatively charged membranes and promoted
372 mightier electrostatic interactions between dissociated functional groups from the
373 material surface. Such electrostatic interactions provoked the shrinking of the
374 membrane material and then, a pore constriction. In parallel, the EfOM in the WWTP
375 secondary effluent became deprotonated at the same circumstances, thus leading to an
376 increase in the accumulation of organic matter on the negatively charged membrane
377 surface and therefore, a higher propensity to be fouled. These results are in accordance
378 with those obtained by other researchers in the same pH range (López-Muñoz et al.,
379 2009; Chang et al., 2011).

380

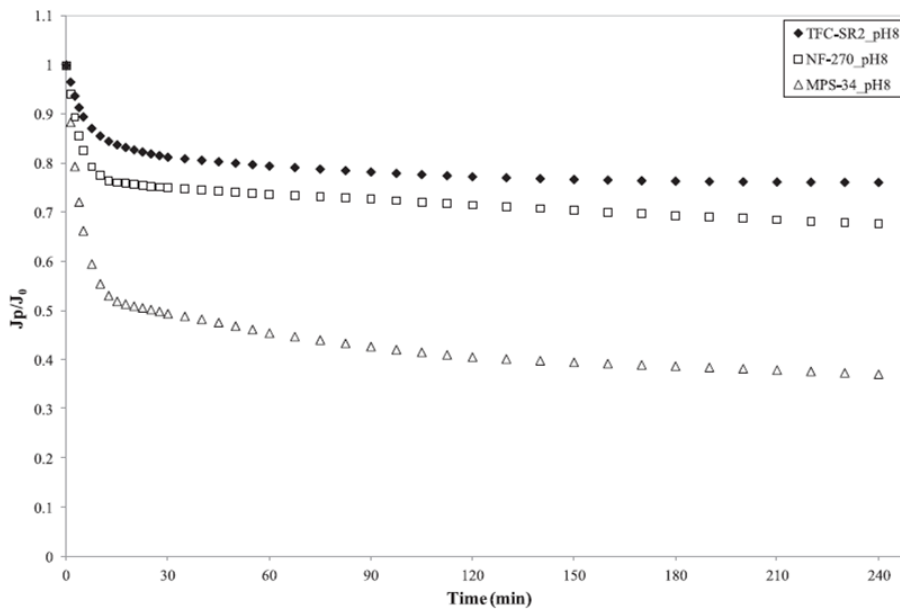


381



(b)

382



(c)

383

Figure 2. Evolution of $J_p(t)/J_0$ over filtration time for each NF membrane at: a) pH 6, b) pH 7, and c) pH 8. Experimental conditions: 5 bar, 500 ± 20 L/h, and 25 ± 2 °C.

384

385

386

387

388

389

390

391

392

393

394

Comparing the results of J_p/J_0 for each membrane, the decline of permeate flux was higher for NF membranes with lower pore size. However, these results should be analyzed carefully. The TFC-SR2 membrane showed the lowest flux decline at each pH value tested (88.02, 77.67 and 76.13% for pH values from 6 to 8, respectively). Despite being a very loose NF membrane, the TFC-SR2 membrane has a relatively high removal of EfOM and a great resistance to fouling phenomena, which is characteristic of the SR series (Nghiem et al., 2006). Several authors reported that the unfouled TFC-SR2 membrane has a water contact angle of about 20-40°, which confirms its higher

395 antifouling character observed in this work (see Table 3). Thus, the higher flux decline
 396 of NF membrane with lowerMWCO cannot be related to the difference of pore size
 397 amongst the selected NF membranes, because of their different surface material, and
 398 can be attributed to the adsorptive interactions between solute molecules in the WWTP
 399 secondary effluent and the polymeric membrane surface. The MPS-34 membrane (a
 400 tight NF membrane) showed the highest flux decline (43.51, 39.93 and 37.09% for pH
 401 6, 7 and 8, respectively). This membrane is made up of polysulfone, which is a semi-
 402 hydrophobic material with low surface charge and water contact angles of about 70-80°,
 403 thus making this membrane more susceptible to be fouled (Fernández et al., 2010;
 404 Dickhout et al., 2017). Such hydrophobic interactions led to cause the sharpest decline
 405 of permeate flux. The NF-270 membrane showed a flux decline in between the two
 406 aforementioned NF membranes. Compared to MPS-34 membranes, the active layer of
 407 the NF-270 membrane is made of polyamide and presents a water contact angle of
 408 around 45° (see Table 3), which demonstrates that NF-270 membranes have a more
 409 hydrophilic character than MPS-34 membranes but less hydrophilic than TFCSR2
 410 membranes.

411

412 The fouling mechanism for each NF membrane at the studied pH range was
 413 assessed using Hermia's model adapted to cross-flow configurations. For the sake of
 414 simplicity, the fitting of the model was evaluated in terms of linear regression
 415 coefficient (R^2), standard deviation (SD) and fitted phenomenological constant
 416 parameter (K). Results of the goodness of data fitting are presented in Table 4.

417

418 **Table 4.** Fitting accuracy of the Hermia's model in terms of R^2 and SD for the selected NF membranes at 25 °C, 5 bar
 419 and 500 ± 20 L/h.

Fouling mechanisms	<u>Gel layer formation</u> n = 0	<u>Incomplete blocking</u> n = 1	<u>Standard blocking</u> n = 1.5	<u>Complete blocking</u> n = 2
$R^2 \pm SD$	pH = 6			
TFC-SR2	0.976 ± 0.005	0.980 ± 0.004	0.782 ± 0.015	0.983 ± 0.004
NF-270	0.961 ± 0.016	0.970 ± 0.014	0.931 ± 0.020	0.977 ± 0.012
MPS-34	0.958 ± 0.028	0.932 ± 0.037	0.182 ± 0.129	0.881 ± 0.049
	pH = 7			
TFC-SR2	0.983 ± 0.009	0.980 ± 0.009	0.676 ± 0.036	0.978 ± 0.009
NF-270	0.962 ± 0.014	0.948 ± 0.016	0.483 ± 0.051	0.934 ± 0.018
MPS-34	0.982 ± 0.025	0.980 ± 0.030	0.258 ± 0.198	0.954 ± 0.051
	pH = 8			
TFC-SR2	0.992 ± 0.006	0.989 ± 0.007	0.388 ± 0.052	0.983 ± 0.008
NF-270	0.973 ± 0.011	0.959 ± 0.013	0.253 ± 0.057	0.942 ± 0.016
MPS-34	0.980 ± 0.031	0.967 ± 0.042	0.487 ± 0.174	0.915 ± 0.069

420

421

Best results for each pH condition and membrane are highlighted in bold.

422

423 It can be observed that gel layer formation, intermediate blocking and complete
 424 blocking were fitted well to the experimental results in all the pH conditions, whereas

425 the standard blocking model showed the poorest fitting among the four fouling
 426 mechanisms and it only fitted well in some cases (e.g. R^2 value of 0.931 ± 0.020 for the
 427 NF-270 membrane at pH 6) but not enough to be considered as the main fouling
 428 mechanism. This indicates that the solute particles did not precipitate on the inner walls
 429 of membrane pores. In the light of the highest degree of model fitness (R^2), the
 430 dominant fouling mechanism was the complete blocking model for both loose TFC-SR2
 431 and NF-270 membranes at pH 6, which means that solute particles completely blocked
 432 pore entrances without penetrating the porous structure. Thus, a monomolecular layer
 433 was formed on the polymeric surface and could act as a secondary barrier for separating
 434 the target emerging contaminants (Corbatón-Báguena et al., 2015a; García-Ivars et al.,
 435 2017). However, gel layer formation became the dominating mechanism at higher pH
 436 levels (see Table 4). In this case, solute particles were accumulated onto the polymeric
 437 surface forming a gel layer but without blocking the pores, which also led to a
 438 formation of a permeable layer on the membrane surface (Corbatón- Báguena et al.,
 439 2015a). As for tight MPS-34 membranes, gel layer formation played the major role in
 440 their fouling at all pH conditions. According to the fitted K values displayed in Table 5
 441 for each NF membrane and each fouling mechanism, the phenomenological constant K
 442 increased at more alkaline pH values, which is consistent with the more severe flux
 443 decline of each membrane at such high pH levels (Fig. 2). Therefore, the predominant
 444 fouling mechanisms during the filtration experiments were the complete blocking model
 445 and the cake layer formation, which could be considered as external mechanisms that
 446 occur on the membrane surface and were more severe for membranes with smaller pore
 447 size (Brião and Tavares, 2012; Corbatón- Báguena et al., 2015b).

448
 449 **Table 5.** Values of model parameter K for each membrane and pH tested.

Fouling mechanisms	Gel layer formation	Incomplete blocking	Standard blocking	Complete blocking
	$n = 0$	$n = 1$	$n = 1.5$	$n = 2$
K	s/m^2	$1/m$	$1/(m^{0.5} \cdot s^{0.5})$	$1/m$
	pH = 6			
TFC-SR2	$0.91 \cdot 10^6$	21.99	$0.24 \cdot 10^{-2}$	21.02
NF-270	$1.49 \cdot 10^6$	24.55	$0.63 \cdot 10^{-2}$	22.15
MPS-34	$283 \cdot 10^6$	445.82	$5.40 \cdot 10^{-2}$	356.29
	pH = 7			
TFC-SR2	$1.19 \cdot 10^6$	26.13	$0.54 \cdot 10^{-2}$	23.67
NF-270	$2.47 \cdot 10^6$	39.28	$0.76 \cdot 10^{-2}$	34.86
MPS-34	$387 \cdot 10^6$	601.28	$8.30 \cdot 10^{-2}$	457.86
	pH = 8			
TFC-SR2	$1.58 \cdot 10^6$	34.35	$0.61 \cdot 10^{-2}$	31.02
NF-270	$3.04 \cdot 10^6$	45.06	$0.80 \cdot 10^{-2}$	40.15
MPS-34	$335 \cdot 10^6$	489.47	$8.60 \cdot 10^{-2}$	354.72

450

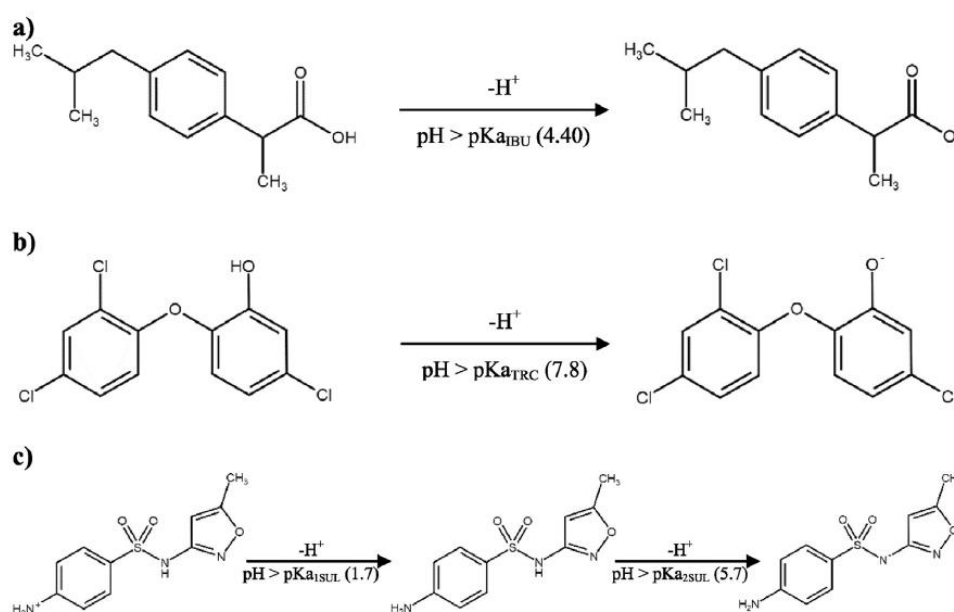
451

452 3.2. Physicochemical properties of the selected PhACs

453

454 The organic compounds selected for this study have low molecular weight with
455 values between 151.17 and 318.14 g/mol (of acetaminophen and diclofenac,
456 respectively). Despite this similarity, these compounds have distinguishing properties
457 that makes them interesting to be compared, including molar volumes, hydrophobicity,
458 dissociation constants, dipole moments and molecular radii (see [Table 2](#)). Regarding the
459 hydrophilic or hydrophobic character of PhACs and the personal care product triclosan,
460 the octanol-water partition coefficient (K_{OW}) can be used as an indicator of the sorption
461 properties of a pollutant, which indicates its hydrophobicity. The organic compounds
462 with a value of $\log K_{OW}$ higher than 2 could be considered as hydrophobic. This
463 parameter is usually considered as pH independent and only reflects hydrophobic
464 interactions, but unlike other properties of target compounds, hydrophobicity is strongly
465 linked to electrostatic interactions, surface complexation or hydrogen bonding, which
466 can significantly change with a variation of pH, especially around the dissociation
467 constant (pK_a). For this reason, a pH-corrected value of $\log K_{OW}$, known as $\log D_{OW}$,
468 can be employed to predict the solute hydrophobicity and it can be defined as the ratio
469 between the ionised and unionised form of the solute at a specific pH value ([Wegst-
470 Uhrich et al., 2014](#)). Both parameters ($\log K_{OW}$ and $\log D_{OW}$) can be useful to describe
471 the sorption potential of a compound in the aquatic environment and have the same
472 value for non-ionisable compounds but substantially differ when the compound is
473 ionisable. This occurs because of the acid-base transformation of the ionisable
474 compounds, which also considerably affects both their solubility and electrostatic nature
475 due to the presence of dissociable functional groups in the organic structures. The
476 groups containing carboxyl or phenols may be deprotonated, thus becoming negatively
477 charged, whereas groups containing amines may be protonated and thus, they gain a
478 positive charge. Such changes in their speciation depend on the characteristic pK_a value
479 of each target compound ([Nghiem and Fujioka, 2016](#)). In general, when the pH of the
480 solution is higher than the intrinsic pK_a value of the target compound, this compound is
481 deprotonated and presents a negative charge. Otherwise, the charge of the organic
482 compound may be neutral or positive or a mixture of both ([Ganiyu et al., 2015](#)). A
483 simple schematic diagram of the speciation of some target compound (ibuprofen,
484 triclosan and sulfamethoxazole) is displayed in [Fig. 3](#). Since the characteristic pK_a
485 values of some target compounds (such as diazepam, diclofenac, ibuprofen, naproxen
486 and sulfamethoxazole) are below the investigated pH range (see [Table 2](#)), these
487 compounds have a negative charge. [Table 6](#) shows the values of $\log D_{OW}$ for each

488 compound at the pH conditions, where caffeine and acetaminophen are hydrophilic (log
 489 $D_{ow} < 1$) throughout the studied pH range while diazepam, diclofenac and triclosan are
 490 highly hydrophobic (log $D_{ow} > 3$). At higher pH values, trimethoprim became more
 491 hydrophobic whereas ibuprofen, naproxen and sulfamethoxazole became more
 492 hydrophilic, being more soluble these compounds in their anionic form, which was
 493 confirmed by other researchers (Nghiem and Hawkes, 2007; Jin et al., 2012). For these
 494 reasons, it can be concluded that the pH of the feed solution has a crucial role in the
 495 application of membrane technology in order to remove emerging contaminants (and
 496 especially PhACs) from wastewater, because both membrane surface and emerging
 497 contaminants properties including solubility, speciation and hydrophobicity are pH
 498 dependent. This influence on the solute rejection will be analysed and discussed in the
 499 following sections.
 500



501
 502 **Figure 3.** Speciation of ibuprofen (a), triclosan (b) and sulfamethoxazole (c).

503
 504

Table 6. Log DOW values obtained for the nine selected PhACs in the tested pH conditions.

Pharmaceutical active compound	pKa	Calculated Log D_{ow} ^a		
		pH 6	pH 7	pH 8
Acetaminophen	9.86	0.91	0.91	0.89
Caffeine	10.40	-0.55	-0.55	-0.55
Diazepam	3.40	3.08	3.08	3.08
Diclofenac	4.08	4.28	4.28	4.28
Ibuprofen	4.40	2.67	1.71	0.85
Naproxen	4.15	1.18	0.25	-0.36
Sulfamethoxazole	5.70	0.60	0.14	-0.11
Triclosan	7.80	4.97	4.90	4.50
Trimethoprim	7.10	0.27	0.92	1.23

^a Software Calculator Plugins was used to calculate Log DOW at each pH.

505
 506

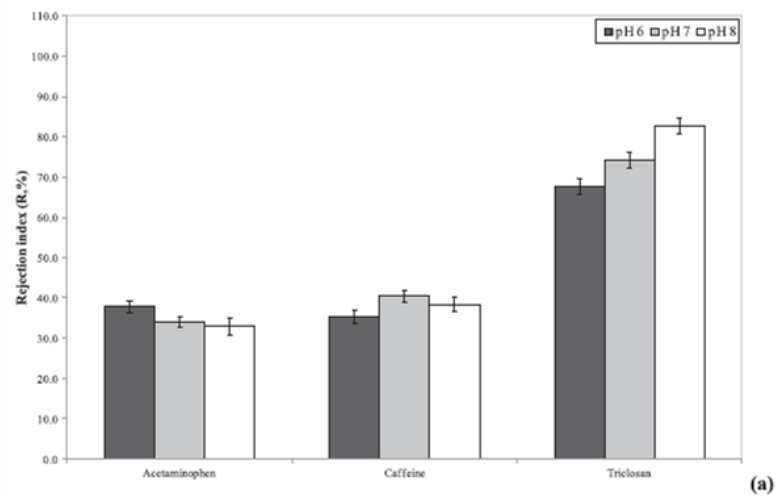
507

508 3.3. Rejection of non-ionic target compounds in WWTP secondary effluent

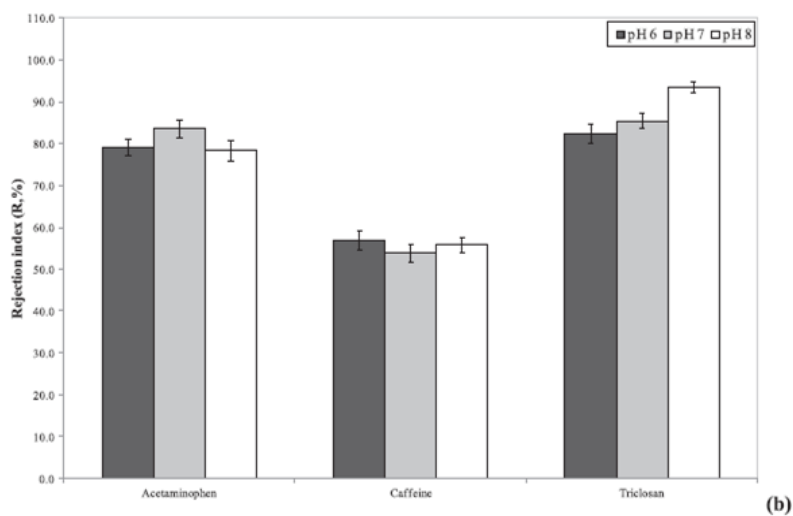
509

510 After analysing the fouling mechanisms of each membrane depending on the
511 operating conditions and the physicochemical properties of the selected organic
512 compounds, the rejection of PhACs and the personal care product triclosan presented
513 in WWTP secondary effluent will be studied, separating charged from uncharged
514 PhACs. Rejection experiments were conducted at different pH values (from 6 to 8) with
515 TFC-SR2, NF-270 and MPS-34 NF membranes. Fig. 4 illustrates the rejection indexes
516 of non-ionic PhACs at the studied pH conditions during the filtration of WWTP
517 wastewater samples for each NF membrane (TFC-SR2, NF-270 and MPS-34).

518



519



520

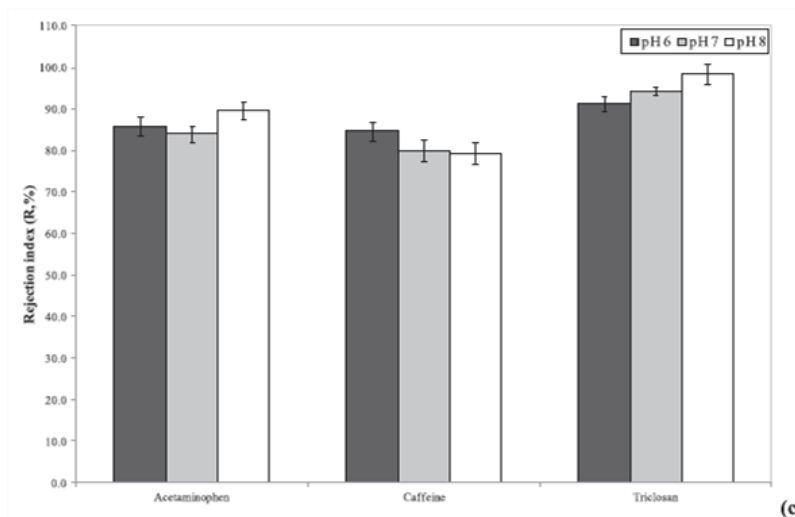


Figure 4. Rejection indexes of non-ionic PhACs at different pHs for each NF membrane: a) TFC-SR2, b) NF-270, and c) MPS-34. Experimental conditions: 5 bar, 500 ± 20 L/h, and 25 ± 2 °C.

521
522
523
524

525 Previously to discuss these results, it must be remarked that triclosan has been
526 included in this figure because this organic compound is uncharged within the pH range
527 except at pH 8, when it becomes negatively charged. For TFC-SR2 membranes (Fig.
528 4a), acetaminophen and caffeine showed similar low removal efficiencies (around 30-
529 40%) at the studied pH conditions, while triclosan presented higher rejection indexes
530 with increasing pH, achieving rejections of more than 80% at pH 8. These differences
531 are strongly related to their distinct molecular weight and hydrophobicity, where
532 acetaminophen and caffeine are hydrophilic ($\log K_{ow} < 1$) and have a lower molecular
533 weight than the MWCO of the selected membranes, whereas triclosan is highly
534 hydrophobic ($\log K_{ow} > 4$) and nearly doubles the size of the molecule of
535 acetaminophen. Comparing these results with those obtained for the NF-270 and MPS-
536 34 membranes (Fig. 4b and c, respectively), rejection indexes of these non-ionic
537 compounds increased with decreasing membrane pore size, classifying the results as
538 follows (from loose to tight structure): $R_{TFC-SR2} < R_{NF-270} < R_{MPS-34}$. Thus, the highest
539 removal efficiencies for non-ionic compounds were observed for the MPS-34
540 membranes which had the tightest structure.

541

542 However, the rejection results observed in Fig. 3 were not only related to the
543 pore size of the membranes and could not consider sieving effect as the main separation
544 mechanism. The impact of membrane fouling on the removal of trace emerging
545 contaminants by using pressure-driven membrane separation processes cannot be
546 neglected, especially for nanofiltration. Generally, the rejection of uncharged trace

547 solutes by NF/RO membranes is considered to be predominantly caused by size
548 exclusion, while the charged trace solutes are mainly rejected by electrostatic
549 interactions with the charged membranes. However, when wastewater is used as feed
550 solution, the existing interactions between non-ionic solutes and membranes may be
551 influenced by EfOM and then, the separation mechanism of uncharged solutes could not
552 be simply attributed to the sieving effect. In this case, hydrophobic interactions that take
553 place between the fouled membrane surface and such solutes gain predominance
554 (Ganiyu et al., 2015). For this reason, although the role of size exclusion in the rejection
555 of triclosan is remarkably observed using NF-270 and MPS-34 membranes, the high
556 removal efficiencies of triclosan can be related to the hydrophobic interactions between
557 the highly hydrophobic triclosan (which has a very high affinity toward both organic
558 matter and polymeric membranes) and the hydrophobic and negatively charged foulant
559 layer formed on the membrane surface due to the adsorption and deposition of organic
560 and inorganic compounds present in WWTP samples, which could act as a second
561 barrier for separation. The formation of this foulant layer onto the membrane surface
562 was demonstrated previously in Section 3.1, where the observed flux decline was
563 attributed to fouling phenomena by EfOM and Hermia's model confirmed that both
564 fouling mechanisms (complete blocking and cake layer formation) are external and
565 occur onto the membrane surface. Moreover, Bellona and his group reported that both
566 TFC-SR2 and NF-270 membranes became more hydrophobic, presenting higher contact
567 angle values when different foulants were accumulated on the fouled membrane surface
568 (Bellona et al., 2010). Therefore, the hydrophobic interactions between triclosan and the
569 formed foulant layer entail a high sorption potential which led to hydrophobic triclosan
570 molecules may be strongly adsorbed on the polymeric surface and also on the additional
571 foulant layer formed onto that surface (Nghiem and Coleman, 2008; Narbaitz et al.,
572 2013).

573

574 Comparing the rejection indexes at different pH conditions, there are some
575 significant differences in the rejection of triclosan with increasing pH, resulting in
576 almost complete rejection at higher pH values. This organic compound existed in both
577 neutral and ionised form within the pH range according to its characteristic pKa value
578 (see Table 2). Triclosan is mostly unionised at pH values lower than its pKa and its non-
579 ionic molecules can be readily complexed with dissolved organic carbon and EfOM
580 molecules (Rowett et al., 2016), while triclosan is mostly ionised at pH 8 (above the

581 pKa value of the compound), becoming a negative species. At these conditions, its
582 rejection was also favoured by the appearance of electrostatic repulsion between
583 compound and membrane. Concerning the behaviour of acetaminophen and caffeine at
584 different pH values, these hydrophilic non-ionic compounds showed to be pH
585 independent with similar values of rejection index at each pH, for a fixed NF
586 membrane. Once the hydrophobic foulant layer is formed, these hydrophilic organic
587 compounds have more affinity for water, thus allowing them to pass through the
588 membrane. However, some molecules from these hydrophilic non-ionic compounds are
589 rejected due to the solute-solute interactions between them and EfOM macromolecules.
590 These solute-solute interactions took place in the effluent and were related to the
591 association of emerging contaminants with EfOM macromolecules, thus forming
592 EfOM-compound complexes as a result of hydrogen bonding and/or electrostatic
593 attraction between the polar moieties of the organic molecules and the functional groups
594 of the EfOM macromolecules, such as the phenolic or carboxylic groups of humic
595 substances-like (Mahlangu et al., 2014; Azaïs et al., 2016). The adsorption of these
596 compounds (humic-like substances) on membrane surfaces can also increase the
597 hydrophobicity of the membrane, as was reported in literature (Nghiem and Coleman,
598 2008; Bellona et al., 2010). Martínez-Hernández and colleagues demonstrated in several
599 sorption experiments with soils that acetaminophen and caffeine showed significant
600 biodegradability in comparison with other PhACs tested (naproxen, carbamazepine and
601 sulfamethoxazole) which resulted in high removal rates (Martínez-Hernández et al.,
602 2016; Martínez-Hernández et al., 2017).

603

604 **3.4. Rejection of ionic target compounds in WWTP secondary effluent**

605

606 **Fig. 5** shows the rejection indexes of charged PhACs during the filtration of the
607 WWTP effluent for TFC-SR2, NF-270 and MPS-34 membranes. The lowest results
608 were obtained for TFC-SR2 membranes (see **Fig. 5a**), where ionic compounds showed
609 medium removal efficiencies at pH 6, achieving values between 45 and 65% (for
610 trimethoprim and diazepam, respectively). This is because the MWCO of TFC-SR2
611 membranes are higher than the molecular weight of the ionic PhACs. These rejection
612 indexes increased up to an average of 65% for almost all the ionic target compounds at
613 pH 8, noting sulfamethoxazole rejection of around 80%. As occurred for non-ionic
614 compounds, removal efficiencies of ionic compounds significantly increased for tighter

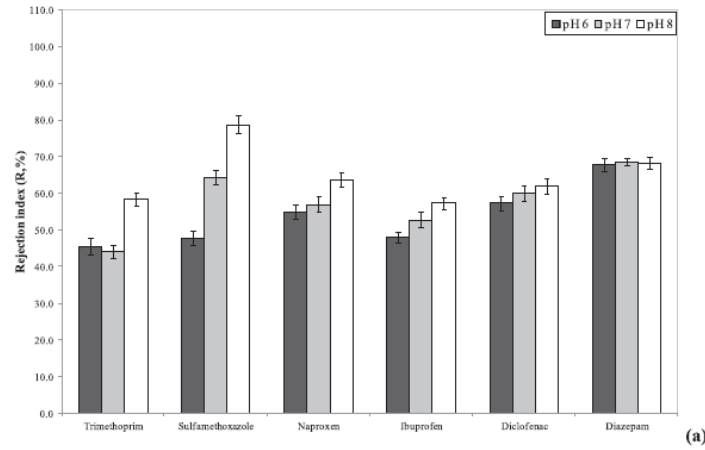
615 membranes, mainly due to size exclusion. The smaller pore size (or MWCO) was, the
616 higher rejection index was obtained. Nevertheless, there is no significant difference
617 between the results of the loose NF-270 membrane and the tight MPS-34 membrane,
618 obtaining very high rejection indexes of ionic compounds with values greater than 90%
619 in the studied pH range for both membranes (which are presented in [Fig. 5b](#) and [c](#)).

620

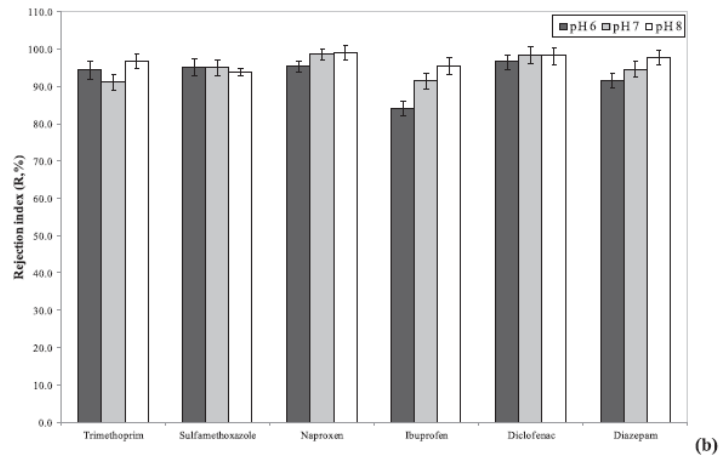
621 However, size exclusion was not the only separation mechanism in the removal
622 of PhACs. These three membranes (TFC-SR2, NF-270 and MPS-34 membranes) were
623 negatively charged under normal pH conditions due to acidic functional groups in the
624 surface structure (as was explained above). In the same way, some PhACs such as
625 diazepam, diclofenac, ibuprofen, naproxen and sulfamethoxazole were anionic
626 compounds in aqueous solutions due to their pK_a values are lower than the studied pH
627 range (see [Table 2](#)), while trimethoprim varied its ionic state at such conditions, being
628 positive at pH 6, neutral at pH 7 and negative at pH 8. Therefore, in addition to size
629 exclusion, the separation mechanism would be governed by electrostatic interactions. It
630 can be observed in [Fig. 5a](#) that diazepam showed similar rejection indexes at the studied
631 pH range for TFC-SR2 membranes. Its negative charge (pK_a_{diazepam} < feed solution pH)
632 indicated that electrostatic repulsion force with the negatively charged membrane
633 surface (and with the formed foulant layer) will be the dominant separation mechanism.
634 Furthermore, the hydrophobicity of diazepam (log D_{OW}: 3.08) could also favour its
635 rejection because its molecules would be partially adsorbed by both the membrane and
636 EfOM macromolecules, especially in proteins ([Bojanić et al., 2011](#); [López-Fernández et
637 al., 2014](#)). Similar behaviour was observed for diclofenac, which presented the highest
638 molecular weight of all target compounds and was highly hydrophobic (log D_{OW}: 4.64)
639 at the studied pH range. Thus, diclofenac possessed a high affinity for the hydrophobic
640 surface and also for the EfOM macromolecules in the feed solution. As occurred with
641 triclosan, the electrostatic repulsion between the deprotonated form of diclofenac and
642 the anionic membrane surfaces together with its high sorption potential (log D_{OW}: 4.64)
643 and high molecular weight, resulted in higher rejection indexes for all NF membranes.
644 In regard to trimethoprim, the rejection indexes were higher when it was charged than
645 when it existed as a non-ionic PhAC. At pH 6 (pK_a_{trimethoprim} < feed solution pH), the
646 positively charged and highly hydrophilic molecules of trimethoprim was significantly
647 rejected due to the electrostatic attraction between this cationic compound and the
648 negatively charged membrane surface (and/or the negative foulant layer formed onto the

649 membrane surface). At the upper limit of the interval (pH 8), trimethoprim molecules
650 with negative charge are less hydrophilic due to its growing $\log D_{OW}$ with increasing
651 alkaline pH values (see [Table 6](#)) and thus, charge repulsion became the main separation
652 mechanism to reject this compound. However, because of its more hydrophobic
653 character, the formation of trimethoprim-EfOM complexes cannot be avoided, thus
654 increasing even more its rejection. The high rejection index observed when
655 trimethoprim existed as a neutral species was predominantly caused by hydrophobic
656 interactions due to the effect of fouling on the membrane. In these conditions, the
657 electrostatic forces ceased to exist and nonionic trimethoprim molecules with low
658 sorption potential ($\log D_{OW} < 2$) were not easily adsorbed by both the hydrophobic
659 membrane surface and the formed foulant layer ([Hajibabania et al., 2011](#); [Jewell et al.,](#)
660 [2016](#)). Ibuprofen, naproxen and sulfamethoxazole showed a more pH-dependent
661 behaviour than the other studied PhACs, presenting higher rejection indexes with
662 increasing pH, which was more visible for TFC-SR2 membranes (see [Fig. 5a](#)) than for
663 both NF-270 and MPS-34 membranes ([Fig. 5b](#) and [c](#), respectively). Despite their
664 different hydrophobicity (ibuprofen and naproxen are hydrophobic while
665 sulfamethoxazole is hydrophilic at neutral pH), these three anionic compounds became
666 more soluble and hydrophilic with increasing pH, presenting $\log D_{OW}$ values lower than
667 1 and hence, decreasing significantly their sorption potential and avoiding the
668 hydrophobic interactions with the foulant layer and also with the NF membrane surface
669 ([Nghiem and Hawkes, 2007](#); [García-Ivars et al., 2017](#)). Furthermore, this rising
670 rejection index could be also attributed to an increase in the negative surface charge of
671 the polymeric NF membranes with increasing pH conditions until reaching the alkaline
672 region, in which a stronger electrostatic repulsion occurred ([López-Muñoz et al., 2009](#)).
673 This was also confirmed for both TFC-SR2 and NF-270 membranes by ([Bellona et al.,](#)
674 [2010](#)), who reported that these fouled membranes slightly became more negatively
675 charged at higher pH conditions. For this reason, it can be concluded that the
676 electrostatic repulsion between these now hydrophilic anionic compounds and the
677 highly negative surface of the polymeric NF membranes and between such compounds
678 and the negative formed foulant layer which acted as a supplementary separation
679 barrier.

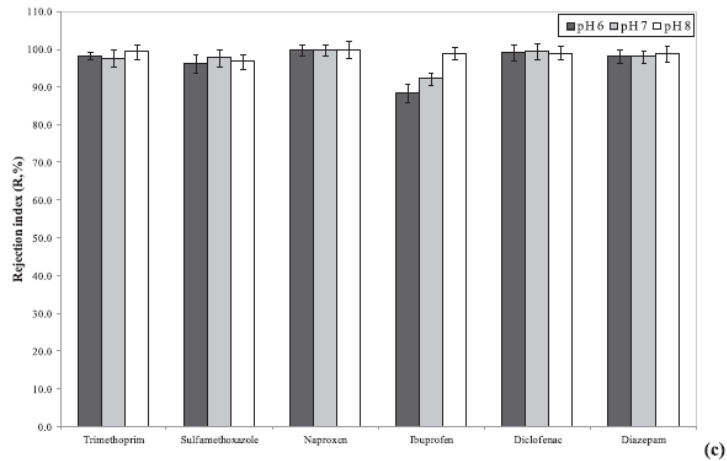
680



681



682



683

684 **Figure 5.** Rejection indexes of charged PhACs at different pHs for each NF membrane: a) TFC-SR2, b) NF-270, and
 685 c) MPS-34. Experimental conditions: 5 bar, 500 ± 20 L/h, and 25 ± 2 °C.

686

687 4. Conclusions

688

689 The role of fouling on the nanofiltration performance at different pH conditions
 690 was elucidated. The flux and rejection of eight selected PhACs with different
 691 physicochemical properties and the personal care product Triclosan by using three spiral

692 wound nanofiltration membranes ranging from loose to tight nanofiltration (classified
693 by size: TFC-SR2 > NF-270 > MPS-34) was studied. The Hermia's model predicted
694 with high accuracy the experimental permeate flux for these three membranes,
695 confirming that the predominant fouling mechanisms were gel layer formation and
696 complete blocking model (the latter was predominant only for TFC-SR2 and NF-270
697 membranes at pH 6). The impact of fouling caused by effluent organic matter on the
698 membrane properties cannot be neglected. Effluent organic matter significantly fouled
699 membranes and was found to be membrane dependent, being especially strong in those
700 with more hydrophobic character. This was observed in both the severe flux decline and
701 the high value of the phenomenological model constant obtained for MPS-34
702 membranes in comparison to those obtained for the other membranes tested (TFC-SR2
703 and NF-270) at the same operating conditions. Fouling heavily influenced the rejection
704 of the nine target compounds due to the formation of a foulant layer onto the membrane
705 surface, which acted as a secondary barrier for separation. This causes an improvement
706 in the electrostatic repulsions between foulant layer/membrane surface and anionic
707 compounds and in the adsorption of non-ionic compounds because of the complexation
708 of emerging contaminants with organic macromolecules in effluent organic matter. At
709 high pH conditions, the propensity for forming this secondary layer significantly
710 improved the size exclusion or sieving mechanism of membranes, thus resulting in
711 higher removal efficiency of some target compounds. The importance of size exclusion
712 or sieving mechanism was observed in the increasing higher rejection indexes achieved
713 with membranes with smaller pore sizes. Thus, the highest removal efficiencies for all
714 the compounds were achieved with MPS-34 membrane which was the tightest
715 nanofiltration membrane selected. The removal efficiencies of target compounds were
716 shown to be mostly dependent on the pH conditions, especially the behaviour of
717 charged target compounds. These ionic compounds presented high rejection indexes at
718 pH, particularly when pH was higher than their characteristic pKa (becoming negative),
719 at which conditions electrostatic repulsion (between the foulant layer and anionic target
720 compounds) and size exclusion were the main separation mechanism. Other compounds
721 such as triclosan and diclofenac showed a high sorption potential, being also rejected
722 due to adsorptive mechanism. In contrast, hydrophilic non-ionic compounds showed a
723 pH-independent behaviour within the studied pH range. For these reasons, it can be
724 concluded that nanofiltration membranes can be a practical tertiary treatment technique
725 to remove emerging contaminants from wastewater effluents, especially for anionic

726 compounds which were highly rejected for membranes with similar pore size to the
727 molecular weights of such target compounds. However, it must take into consideration
728 the generation of a waste stream with a high content of target compounds and inorganic
729 and organic matter, which should be managed in a sustainable way.

730

731

732 **Acknowledgements**

733

734 The authors thank the financial support from the Spanish Ministry of Economy and
735 Competitiveness through the project CTM2013-42342-P. Likewise, the authors also
736 express their acknowledge to the personnel of the Carraixet WWTP for the kind supply
737 of secondary effluent samples.

738

739 **References**

740

741 [Ali Zazouli, M., Susanto, H., Nasser, S., Ulbricht, M., 2009. Influences of solution
742 chemistry and polymeric natural organic matter on the removal of aquatic
743 pharmaceutical residuals by nanofiltration. *Water Res.* 43, 3270-3280.](#)

744

745 [Al-Rashdi, B.A.M., Johnson, D.J., Hilal, N., 2013. Removal of heavy metal ions by
746 nanofiltration. *Desalination* 315, 2-17.](#)

747

748 [Altmann, J., Ruhl, A.S., Zietzschmann, F., Jekel, M., 2014. Direct comparison of
749 ozonation and adsorption onto powdered activated carbon for micropollutant removal in
750 advanced wastewater treatment. *Water Res.* 55, 185-193.](#)

751

752 [American Public Health Association \(APHA\), 2012. Standard Methods for the
753 Examination of Water and Wastewater, twenty-second ed. Washington, DC.](#)

754

755 [Archer, E., Petrie, B., Kasprzyk-Hordern, B., Wolfaardt, G.M., 2017. The fate of
756 pharmaceuticals and personal care products \(PPCPs\), endocrine disrupting contaminants
757 \(EDCs\), metabolites and illicit drugs in a WWTW and environmental waters.
758 *Chemosphere* 174, 437-446.](#)

759

760 Avdeef, A., Nielsen, P.E., Tsinman, O., 2004. PAMPA-a drug absorption in vitro model
761 11. Matching the in vivo unstirred water layer thickness by individual-well stirring in
762 microtitre plates. *Eur. J. Pharm. Sci.* 22, 365-374.
763

764 Azaïs, A., Mendret, J., Gassara, S., Petit, E., Deratani, A., Brosillon, S., 2014.
765 Nanofiltration for wastewater reuse: counteractive effects of fouling and matrice on the
766 rejection of pharmaceutical active compounds. *Sep. Purif. Technol.* 133, 313-327.
767

768 Azaïs, A., Mendret, J., Petit, E., Brosillon, S., 2016. Evidence of solute-solute
769 interactions and cake enhanced concentration polarization during removal of
770 pharmaceuticals from urban wastewater by nanofiltration. *Water Res.* 104, 156-167.
771

772 Bellona, C., Marts, M., Drewes, J.E., 2010. The effect of organic membrane fouling on
773 the properties and rejection characteristics of nanofiltration membranes. *Sep. Purif.*
774 *Technol.* 74, 44-54.
775

776 Bojanić, Z., Bojanić, N., Bojanić, V., Lazović, M., 2011. Drug interactions with
777 diazepam. *Acta Medica Median.* 50 (2), 76-82.
778

779 Brião, V.B., Tavares, C.R.G., 2012. Pore blocking mechanism for the recovery of milk
780 solids from dairy wastewater by ultrafiltration. *Braz. J. Chem. Eng.* 29, 393-407.
781

782 Carbonell-Alcaina, C., Corbatón-Báguena, M.J., Álvarez-Blanco, S., Bes-Piá, M.A.,
783 Mendoza-Roca, J.A., Pastor-Alcañiz, L., 2016. 2016. Determination of fouling
784 mechanisms in polymeric ultrafiltration membranes using residual brines from table
785 olive storage wastewaters as feed. *J. Food Eng.* 187, 14-23.
786

787 Carmona, E., Andreu, V., Picó, Y., 2014. Occurrence of acidic pharmaceuticals and
788 personal care products in Turia river basin: from waste to drinking water. *Sci. Total*
789 *Environ.* 484, 53-63.
790

791 Chang, E.E., Yang, S.Y., Huang, C.P., Liang, C.H., Chiang, P.C., 2011. Assessing the
792 fouling mechanisms of high-pressure nanofiltration membrane using the modified
793 Hermia model and the resistance-in-series model. *Sep. Purif. Technol.* 79, 329-336.

794

795 Chon, K., Cho, J., Shon, H.K., 2013. A pilot-scale hybrid municipal wastewater
796 reclamation system using combined coagulation and disk filtration, ultrafiltration, and
797 reverse osmosis: removal of nutrients and micropollutants, and characterization of
798 membrane foulants. *Bioresour. Technol.* 141, 109-116.

799

800 Chon, K., Chon, K., Cho, J., 2017. Characterization of size fractionated dissolved
801 organic matter from river water and wastewater effluent using preparative high
802 performance size exclusion chromatography. *Org. Geochem.* 103, 105-112.

803

804 Comerton, A.M., Andrews, R.C., Bagley, D.M., 2009. The influence of natural organic
805 matter and cations on the rejection of endocrine disrupting and pharmaceutically active
806 compounds by nanofiltration. *Water Res.* 43, 613-622.

807

808 Corbatón-Báguena, M.J., Gugliuzza, A., Cassano, A., Mazzei, R., Giorno, L., 2015a.
809 Destabilization and removal of immobilized enzymes adsorbed onto polyethersulfone
810 ultrafiltration membranes by salt solutions. *J. Membr. Sci.* 486, 207-214.

811

812 Corbatón-Báguena, M.J., Álvarez-Blanco, S., Vincent-Vela, M.C., 2015b. Fouling
813 mechanisms of ultrafiltration membranes fouled with whey model solutions.
814 *Desalination* 360, 87-96.

815

816 Corbatón-Báguena, M.J., Vincent-Vela, M.C., Gozávez-Zafrilla, J.M., Álvarez-Blanco,
817 S., Lora-García, J., Catalán-Martínez, D., 2016. Comparison between artificial neural
818 networks and Hermia's models to assess ultrafiltration performance. *Sep. Purif.*
819 *Technol.* 170, 434-444.

820

821 De Munari, A., Correia Semiao, A.J., Antizar-Ladislao, B., 2013. Retention of pesticide
822 Endosulfan by nanofiltration: influence of organic matter-pesticide complexation and
823 solute-membrane interactions. *Water Res.* 47, 3484-3496.

824

825 Dickhout, J.M., Moreno, J., Biesheuvel, P.M., Boels, L., Lammertink, R.G.H., de Vos,
826 W.M., 2017. Produced water treatment by membranes: a review from a colloidal
827 perspective. *J. Colloid Interf. Sci.* 487, 523-534.

828

829 Dolar, D., Košutić, K., Ašperger, D., 2013. Influence of adsorption of pharmaceuticals
830 onto RO/NF membranes on their removal from water. *Water Air Soil Pollut.* 224, 1377-
831 1390.

832

833 Dražević, E., Košutić, K., Dananić, V., Pavlović, D.M., 2013. Coating layer effect on
834 performance of thin film nanofiltration membrane in removal of organic solutes. *Sep.*
835 *Purif. Technol.* 118, 530-539.

836

837 Fernández, P., Riera, F.A., Álvarez, R., Álvarez, S., 2010. Nanofiltration regeneration
838 of contaminated single-phase detergents used in the dairy industry. *J. Food Eng.* 97,
839 319-328.

840

841 Field, R.W., Wu, D., Howell, J.A., Gupta, B.B., 1995. Critical flux concept for
842 microfiltration fouling. *J. Membr. Sci.* 100, 259-272.

843

844 Ganiyu, S.O., Van Hullebusch, E.D., Cretin, M., Esposito, G., Otturan, M.A., 2015.
845 Coupling of membrane filtration and advanced oxidation processes for removal of
846 pharmaceutical residues: a critical review. *Sep. Purif. Technol.* 156, 891-914.

847

848 García-Ivars, J., Durá-María, J., Moscardó-Carreño, C., Carbonell-Alcaina, C., Alcaina-
849 Miranda, M.I., Iborra-Clar, M.I., 2017. Rejection of trace pharmaceutically active
850 compounds present in municipal wastewaters using ceramic fine ultrafiltration
851 membranes: effect of feed solution pH and fouling phenomena. *Sep. Purif. Technol.*
852 175, 58-71.

853

854 Gracia-Lor, E., Sancho, J.V., Serrano, R., Hernández, F., 2012. Occurrence and removal
855 of pharmaceuticals in wastewater treatment plants at the Spanish Mediterranean area of
856 Valencia. *Chemosphere* 87, 453-462.

857

858 Grandclément, C., Seyssiecq, I., Piram, A., Wong-Wah-Chung, P., Vanot, G., Tiliacos,
859 N., Roche, N., Doumenq, P., 2017. From the conventional biological wastewater
860 treatment to hybrid processes, the evaluation of organic micropollutant removal: a
861 review. *Water Res.* 111, 297-317.

862

863 Hajibabania, S., Verliefde, A., Drewes, J.E., Nghiem, L.D., McDonald, J., Khan, S., Le-
864 Clech, P., 2011. Effect of fouling on removal of trace organic compounds by
865 nanofiltration. *Water Eng. Sci.* 4, 71-82.

866

867 Halling-Sorensen, B., Nors Nielsen, S., Lanzsky, P., Ingerslev, F., Holten Lützhøft, H.,
868 Jørgensen, S., 1998. Occurrence, fate and effects of pharmaceutical substances in the
869 environment-a review. *Chemosphere* 36, 357-393.

870

871 Heberer, T., 2002. Occurrence, fate, and removal of pharmaceutical residues in the
872 aquatic environment: a review of recent research data. *Toxicol. Lett.* 131, 5-17.

873

874 Hermia, J., 1982. Constant pressure blocking filtration laws e application to powerlaw
875 non-newtonian fluids. *Trans. IChemE* 60, 183-187.

876

877 Jermann, D., Pronk, W., Boller, M., Schöfer, A.I., 2009. The role of NOM fouling for
878 the retention of estradiol and ibuprofen during ultrafiltration. *J. Membr. Sci.* 329, 75-84.

879

880 Jewell, K.S., Castronovo, S., Wick, A., Falas, P., Joss, A., Ternes, T.A., 2016. New
881 insights into the transformation of trimethoprim during biological wastewater treatment.
882 *Water Res.* 88, 550-557.

883

884 Jin, X., Shan, J., Wang, C., Wei, J., Tang, C.Y., 2012. Rejection of pharmaceuticals by
885 forward osmosis membranes. *J. Hazard. Mater.* 227e228, 55-61.

886

887 Jung, C., Son, A., Her, N., Zoh, K.D., Cho, J., Yoon, Y., 2015. Removal of endocrine
888 disrupting compounds, pharmaceuticals, and personal care products in water using
889 carbon nanotubes: a review. *J. Ind. Eng. Chem.* 27, 1-11.

890

891 Katsoyiannis, I.A., Gkotsis, P., Castellana, M., Cartechini, F., Zouboulis, A.I., 2017.
892 Production of demineralized water for use in thermal power stations by advanced
893 treatment of secondary wastewater effluent. *J. Environ. Manage* 190, 132-139.

894

895 Khansary, M.A., Mellat, M., Saadat, S.H., Ramandi, M.F., Kamali, M., Taheri, R.A.,
896 2017. An enquiry on appropriate selection of polymers for preparation of polymeric
897 nanosorbents and nanofiltration/ultrafiltration membranes for hormone micropollutants
898 removal from water effluents. *Chemosphere* 168, 91-99.
899

900 Kochkodan, V., Hilal, N., 2015. A comprehensive review on surface modified polymer
901 membranes for biofouling mitigation. *Desalination* 356, 187e207.
902

903 Li, Q., Elimelech, M., 2004. Organic fouling and chemical cleaning of nanofiltration
904 membranes: measurements and mechanisms. *Environ. Sci. Technol.* 38, 4683-4693.
905

906 Lin, J., Tang, C.Y., Huang, C., Tang, Y.P., Ye, W., Li, J., Shen, J., Van den Broeck, R.,
907 Van Impe, J., Volodin, A., Van Haesendonck, C., Sotto, A., Luis, P., Van der Bruggen,
908 B., 2016. A comprehensive physico-chemical characterization of superhydrophilic loose
909 nanofiltration membranes. *J. Membr. Sci.* 501, 1-14.
910

911 Lin, Y.-L., Chiou, J.-H., Lee, C.-H., 2014. Effect of silica fouling on the removal of
912 pharmaceuticals and personal care products by nanofiltration and reverse osmosis
913 membranes. *J. Hazard. Mater.* 277, 102-109.
914

915 López-Fernández, R., McDonald, J.A., Khan, S.J., Le-Clech, P., 2014. Removal of
916 pharmaceuticals and endocrine disrupting chemicals by a submerged membrane
917 photocatalysis reactor (MPR). *Sep. Purif. Technol.* 127, 131-139.
918

919 López-Muñoz, M.J., Sotto, A., Arsuaga, J.M., Van der Bruggen, B., 2009. Influence of
920 membrane, solute and solution properties on the retention of phenolic compounds in
921 aqueous solution by nanofiltration membranes. *Sep. Purif. Technol.* 66, 194-201.
922

923 Mahlangu, T.O., Hoek, E.M.V., Mamba, B.B., Verliefde, A.R.D., 2014. Influence of
924 organic, colloidal and combined fouling on NF rejection of NaCl and carbamazepine:
925 role of solute-foulant-membrane interactions and cake-enhanced concentration
926 polarisation. *J. Membr. Sci.* 471, 35-46.
927

928 Martínez-Hernández, V., Meffe, R., Herrera-López, S., de Bustamante, I., 2016. The
929 role of sorption and biodegradation in the removal of acetaminophen, carbamazepine,
930 caffeine, naproxen and sulfamethoxazole during soil contact: a kinetics study. *Sci. Total*
931 *Environ.* 559, 232-241.

932

933 Martínez-Hernández, V., Meffe, R., Kohfahl, C., de Bustamante, I., 2017. Investigation
934 natural attenuation of pharmaceuticals through unsaturated column testes. *Chemosphere*
935 177, 292-302.

936

937 Miralles-Cuevas, S., Oller, I., Agüera, A., Sánchez-Pérez, J.A., Malato, S., 2017.
938 Strategies for reducing cost by using solar photo-Fenton treatment combined with
939 nanofiltration to remove microcontaminants in real municipal effluents: toxicity and
940 economic assessment. *Chem. Eng. J.* 318, 161-170.

941

942 Narbaitz, R.M., Rana, D., Dong, H.T., Morrissette, J., Matsuura, T., Jasim, S.Y., Tabe,
943 S., Yang, P., 2013. Pharmaceutical and personal care products removal from drinking
944 water by modified cellulose acetate membrane: field testing. *Chem. Eng. J.* 225, 848-
945 856.

946

947 Nghiem, L.D., Coleman, P.J., 2008. NF/RO filtration of the hydrophobic ionogenic
948 compound triclosan: transport mechanisms and the influence of membrane fouling. *Sep.*
949 *Purif. Technol.* 62, 709-716.

950

951 Nghiem, L.D., Fujioka, T., 2016. Removal of emerging contaminants for water reuse by
952 membrane technology. In: Singh, R., Hankins, N. (Eds.), *Emerging Membrane*
953 *Technology for Sustainable Water Treatment*. Elsevier Science, Oxford, pp. 217-247.

954

955 Nghiem, L.D., Hawkes, S., 2007. Effects of membrane fouling on the nanofiltration of
956 pharmaceutically active compounds (PhACs): mechanisms and role of membrane pore
957 size. *Sep. Purif. Technol.* 57, 176-184.

958

959 Nghiem, L.D., Schäfer, A.I., Elimelech, M., 2006. Role of electrostatic interactions in
960 the retention of pharmaceutically active contaminants by a loose nanofiltration
961 membrane. *J. Membr. Sci.* 286, 52e59.

962

963 Owusu-Agyeman, I., Jeihanipour, A., Luxbacher, T., Schöfer, A.I., 2017. Implications
964 of humic acid, inorganic carbon and speciation on fluoride retention mechanisms in
965 nanofiltration and reverse osmosis. *J. Membr. Sci.* 528, 82-94.

966

967 Pascual-Aguilar, J., Andreu, V., Gimeno-García, E., Picó, Y., 2015. Current
968 anthropogenic pressures on agro-ecological protected coastal wetlands. *Sci. Total.*
969 *Environ.* 503-504, 190-199.

970

971 Petrie, B., Barden, R., Kasprzyk-Hordern, B., 2015. A review on emerging
972 contaminants in wastewaters and the environment: current knowledge, understudied
973 areas and recommendations for future monitoring. *Water Res.* 72, 3-27.

974

975 Picó, Y., Barceló, D., 2015. Transformation products of emerging contaminants in the
976 environment and high-resolution mass spectrometry: a new horizon. *Anal. Bioanal.*
977 *Chem.* 407, 6257-6273.

978

979 Rowett, C.J., Hutchinson, T.H., Comber, S.D.W., 2016. The impact of natural and
980 anthropogenic dissolved organic carbon (DOC), and pH on the toxicity of triclosan to
981 the crustacean *Gammarus pulex* (L.). *Sci. Total. Environ.* 565, 222-231.

982

983 Schmidt, S., Winter, J., Gallert, C., 2012. Long-term effects of antibiotics on the
984 elimination of chemical oxygen demand, nitrification, and viable bacteria in laboratory-
985 scale wastewater treatment plants. *Arch. Environ. Contam. Toxicol.* 63, 354-364.

986

987 Smith Jr., J.S., 2014. Chapter 3: presence and fate of pharmaceuticals in the
988 environment and in drinking water. In: Goldstein, Walter E. (Ed.), *Pharmaceutical*
989 *Accumulation in the Environment: Prevention, Control, Health Effects, and Economic*
990 *Impact*, first ed. CRC Press, USA, pp. 21-42.

991

992 Snyder, S.A., Adham, S., Redding, A.M., Cannon, F.S., DecCarolis, J., Oppeneimer, J.,
993 Wert, E.C., Yoon, Y., 2007. Role of membranes and activated carbon in the removal of
994 endocrine disruptors and pharmaceuticals. *Desalination* 202, 156-181.

995

996 Van der Bruggen, B., Mänttari, M., Nyström, M., 2008. Drawbacks of applying
997 nanofiltration and how to avoid them: a review. *Sep. Purif. Technol.* 63, 251-263.
998

999 Vazquez-Roig, P., Andreu, V., Onghena, M., Blasco, C., Pic_o, Y., 2011. Assessment
1000 of the occurrence and distribution of pharmaceuticals in a Mediterranean wetland
1001 (L'Albufera, Valencia, Spain) by LC-MS/MS. *Anal. Bioanal. Chem.* 400, 1287-1301.
1002

1003 Vergili, I., 2013. Application of nanofiltration for the removal of carbamazepine,
1004 diclofenac and ibuprofen from drinking water sources. *J. Environ. Manage* 127, 177-
1005 187.
1006

1007 Verlicchi, P., Al Aukidy, M., Zambello, E., 2012. Occurrence of pharmaceutical
1008 compounds in urban wastewater: removal, mass load and environmental risk after a
1009 secondary treatment e a review. *Sci. Total Environ.* 429, 123-155.
1010

1011 Verlicchi, P., Zambello, E., 2015. Pharmaceuticals and personal care products in
1012 untreated and treated sewage sludge: occurrence and environmental risk in the case of
1013 application on soil e a critical review. *Sci. Total Environ.* 538, 750-767.
1014

1015 Vincent-Vela, M.C., _Alvarez-Blanco, S., Lora-García, J., Bergantinos-Rodríguez, E.,
1016 2009. Analysis of membrane pore blocking models adapted to cross-flow ultrafiltration
1017 in the ultrafiltration of PEG. *Chem. Eng. J.* 149, 232-241.
1018

1019 Wang, J., Wang, S., 2016. Removal of pharmaceuticals and personal care products
1020 (PPCPs) from wastewater: a review. *J. Environ. Manage* 182, 620-640.
1021

1022 Wegst-Uhrich, S.R., Navarro, D.A.G., Zimmermann, L., Aga, D.S., 2014. Assessing
1023 antibiotic sorption in soil: a literature review and new case studies on sulfonamides and
1024 macrolides. *Chem. Cent. J.* 8, 5.
1025

1026 Yangali-Quintanilla, V., Sadmani, A., McConville, M., Kennedy, M., Amy, G., 2009.
1027 Rejection of pharmaceutically active compounds and endocrine disrupting compounds
1028 by clean and fouled nanofiltration membranes. *Water Res.* 43, 2349-2362.
1029

1030 Yangali-Quintanilla, V., Sadmani, A., McConville, M., Kennedy, M., Amy, G., 2010. A
1031 QSAR model for predicting rejection of emerging contaminants (pharmaceuticals,
1032 endocrine disruptors) by nanofiltration membranes. *Water Res.* 44, 373-384.

1033

1034 **List of symbols**

1035

1036 Variables

1037

1038	A_m :	Effective area of the membrane (m ²)
1039	C_f :	Concentration of each pharmaceutically active compound in the feed 1040 stream (ng/L)
1041	C_p :	Concentration of each pharmaceutically active compound in the permeate 1042 stream (ng/L)
1043	D_{OW} :	pH-dependent octanol-water distribution coefficient (dimensionless)
1044	D_S :	Diffusion coefficient of an organic compound in water (m ² /s)
1045	J_0 :	Initial permeate flux (L/m ² ·h)
1046	J_p :	Permeate flux (L/m ² ·h)
1047	J_{pss} :	Steady-state permeate flux (L/m ² ·h)
1048	K :	Phenomenological model constant (units depending on n)
1049	k_B :	Boltzmann constant (kg·m ² /(K·s ²))
1050	K_{OW} :	Octanol-water partition coefficient (dimensionless)
1051	LOD :	Limit of detection (ng/L)
1052	LOQ :	Limit of quantification (ng/L)
1053	M_{DIP} :	Dipole moment (D or Debyes)
1054	M_w :	Molecular weight of a compound (g/mol)
1055	$MWCO$:	Molecular weight cut-off of a membrane (Da)
1056	n :	Model parameter (dimensionless)
1057	pKa :	Dissociation constant (dimensionless)
1058	R :	Solute rejection index (%)
1059	R^2 :	Linear regression coefficient (dimensionless)
1060	r_s :	Molecular radius or Stokes radius (m)
1061	SD :	Standard deviation (dimensionless)
1062	t :	Filtration time (h)
1063	T :	Temperature (K)

1064	<i>V</i> :	Total volume permeated during an experimental time interval (L)
1065	<i>V_s</i> :	Molar volume of a compound (cm ³ /s)
1066	ΔP :	Transmembrane pressure (bar)
1067	<i>h</i> :	Water viscosity (kg/(m·s))
1068		
1069	Abbreviations	
1070		
1071	<i>COD</i> :	Chemical oxygen demand
1072	<i>EfOM</i> :	Effluent organic matter
1073	<i>HPLC</i> :	High-performance liquid chromatography
1074	<i>HPLC-MS/MS</i> :	High-performance liquid chromatography tandem-mass spectrometry
1075	<i>NF</i> :	Nanofiltration
1076	<i>NOM</i> :	Natural organic matter
1077	<i>PhAC</i> :	Pharmaceutically active compound
1078	<i>RO</i> :	Reverse osmosis
1079	<i>SPE</i> :	Solid-phase extraction
1080	<i>UF</i> :	Ultrafiltration
1081	<i>WWTP</i> :	Wastewater treatment plant